

ANALYSIS OF THE $B^{0(+)} \rightarrow J/\psi D^{0(+)}$ DECAYS*M. Sayahi¹, H. Mehraban²*

Physics Department, Semnan University, Semnan, Iran

We analyze $B^{0(+)} \rightarrow J/\psi D^{0(+)}$ decays by considering the contributions of annihilation diagrams. For each diagram, we calculate the branching ratios for various parameters X_A , which have played a significant role in our results. These parameters have been concluded from the divergence integrals in hard-scattering kernels. Here, we have considered three effective variables, including: $\Lambda(225, 500 \text{ MeV})$, $\rho_A(0, 1, 1/2)$, and φ_A . It is found that the most of the obtained data are placed in the experimental range at $\Lambda = 225 \text{ MeV}$ and $\Lambda = 500 \text{ MeV}$ for $B^+ \rightarrow J/\psi D^+$ and $B^0 \rightarrow J/\psi D^0$, respectively.

Проводится анализ распадов $B^{0(+)} \rightarrow J/\psi D^{0(+)}$ при учете вкладов аннигиляционных диаграмм. Для каждой из диаграмм приводятся соотношения брэнчинга для различных переменных X_A , которые играют важную роль при получении приводимых результатов. Подобные параметры можно получить из расходящихся интегралов в процессах жесткого рассеяния ядер. Были исследованы три следующие эффективные переменные: $\Lambda(225, 500 \text{ МэВ})$, $\rho_A(0, 1, 1/2)$ и φ_A . Показано, что большая часть полученных данных находится в экспериментальной области, если взять $\Lambda = 225 \text{ МэВ}$ и $\Lambda = 500 \text{ МэВ}$ для $B^+ \rightarrow J/\psi D^+$ и $B^0 \rightarrow J/\psi D^0$ соответственно.

PACS: 13.25.Hw; 12.38.Bx

INTRODUCTION

The nonleptonic charmless decay channels $B \rightarrow M_1 M_2$ provide some information about CP violation and strong interactions. There are some ways to obtain decay rates and CP asymmetries with QCD effects. The task is simplified by the use of soft collinear effective theory (SCET), QCD factorization (QCDF), and perturbative QCD (pQCD) to calculate hadronic-decay amplitudes. The factorization theorems for $B \rightarrow M_1 M_2$ amplitudes were derived with an expansion in Λ/Q , where Λ is a hadronic scale and $Q \sim m_b$ [1]. The annihilation amplitudes are power suppressed by order Λ_{QCD}/m_b . In the QCD factorization method, the annihilation contributions do not appear. It is because of the endpoint divergence. But in some of B -meson decays, these contributions are numerically important. Weak annihilation effects are not similar to hard spectator interactions. Since they have endpoint singularities at twist-2 order in the light-cone expansion for the final-state mesons and by ignoring the soft endpoint divergence, the annihilation contributions have been written in terms of convolutions of hard-scattering kernels with light-cone distribution amplitudes, including the chirally enhanced twist-3 projections [2]. In this paper, we have studied $B^+ \rightarrow J/\psi D^+$ and $B^0 \rightarrow J/\psi D^0$ decays by considering the contributions of annihilation diagrams. For the last decay, $B^0 \rightarrow J/\psi D^0$, the branching ratio is calculated in pQCD approach which is given to be $(3.45_{-1.46}^{+1.22} \pm 1.51 \pm 0.32) \cdot 10^{-6}$ [3].

¹E-mail: m_sayahi@sun.semnan.ac.ir²E-mail: hmehraban@semnan.ac.ir

1. THE ANNIHILATION CONTRIBUTIONS FOR $B \rightarrow VP$ DECAYS

1.1. $B^{0(+)} \rightarrow J/\psi D^{0(+)}$ Decays. The effective Hamiltonian for $B \rightarrow M_1 M_2$ decays can be written generally as

$$H_{\text{eff}} = \frac{G_F}{\sqrt{2}} \sum_{p=u,c} \lambda_p^D \left(C_1 O_1^p + C_2 O_2^p + \sum_{i=3}^{10} C_i O_i \right) + \text{h.c.}, \quad (1)$$

where $\lambda_p^D = V_{pb} V_{pD}^*$ ($D = d, s$) are the products of CKM elements and C_i s are the Wilson coefficients in NDR scheme. G_F is the Fermi constant. The matrix elements of the weak effective Hamiltonian can be written as

$$\langle M_1 M_2 | H_{\text{eff}} | B \rangle = \frac{G_F}{\sqrt{2}} \sum_{p=u,c} \lambda_p \langle M_1 M_2 | T_p + T_{\text{ann}} | B \rangle. \quad (2)$$

The matrix elements of the operators in T_p are factorized into two currents, which are form factor and decay constant including the coefficients a_i in factorization approach. The other term, e.g., T_{ann} , is the weak annihilation contribution and introduces a set of coefficients b_i . The decay amplitude of weak annihilation effects is given by

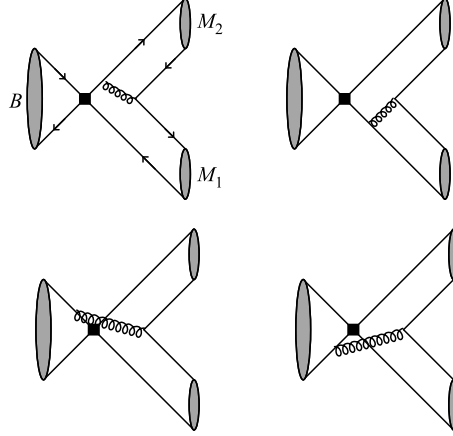
$$A_{\text{ann}} = \frac{G_F}{\sqrt{2}} \lambda_p \langle M_1 M_2 | T_{\text{ann}} | B \rangle = \frac{G_F}{\sqrt{2}} f_B f_{M_1} f_{M_2} b_i^p(M_1 M_2), \quad (3)$$

where f_B , f_{M_1} , and f_{M_2} are decay constants of mesons in decay. We consider only diagrams proportional to α_s and use the convention that M_1 contains an antiquark from the weak vertex with longitudinal momentum fraction \bar{y} . For nonsinglet annihilation, M_2 contains a quark from the weak vertex with momentum fraction x [4]. There are four weak annihilation diagrams in Fig. 1. Weak annihilation is parameterized by a set of coefficients $b_i^p(VP)$:

$$\begin{aligned} b_1 &= \frac{C_F}{N_c^2} C_1 A_1^i, \\ b_2 &= \frac{C_F}{N_c^2} C_2 A_1^i, \\ b_3^p &= \frac{C_F}{N_c^2} [C_3 A_1^i + C_5 (A_3^i + A_3^f) + N_c C_6 A_3^f], \\ b_4^p &= \frac{C_F}{N_c^2} [C_4 A_3^i + C_6 A_2^i], \\ b_{3,\text{EW}}^p &= \frac{C_F}{N_c^2} [C_9 A_1^i + C_7 (A_3^i + A_3^f) + N_c C_8 A_3^f], \\ b_{4,\text{EW}}^p &= \frac{C_F}{N_c^2} [C_{10} A_1^i + C_8 A_2^i]. \end{aligned} \quad (4)$$

The superscripts i, f refer to gluon emission from the initial- and final-state quarks, respectively, and they refer to Dirac structures. (b_1, b_2) , (b_3, b_4) , and $(b_{3,\text{ew}}, b_{4,\text{ew}})$ are related to the current-current, the penguin and the electroweak penguin annihilation structures.

We can take the infinite mass limit of b quark in which m_b goes to infinity while $m_{J/\psi}$ is fixed ($m_{J/\psi}/m_b \rightarrow 0$). So, we assume that J/ψ behaves as a light meson, due to its size, and


 Fig. 1. The annihilation diagrams for $B \rightarrow M_1 M_2$

we can describe light-cone distribution amplitude for J/ψ . Also, we treat the charm quark as light compared to the large scale provided by the mass of the decaying b quark ($m_c \ll m_b$ and m_c fixed as $m_b \rightarrow \infty$), and we use a light-cone projection similar to that of light mesons also for the D meson. In addition, we assume that m_c is still large compared to Λ_{QCD} . Then we have used annihilation formula for $B \rightarrow M_1 M_2$ decay, where M_2 is a vector meson and M_1 is a pseudoscalar. Then we have

$$\begin{aligned}
 A_1^i &= \pi\alpha_s \int_0^1 dx dy \left[\phi_V(x)\phi_P(y) \left[\frac{1}{y(1-\bar{x}y)} + \frac{1}{y\bar{x}^2} \right] + r_\chi^V r_\chi^P \phi_v(x)\phi_p(y) \frac{2}{y\bar{x}} \right], \\
 A_2^i &= -\pi\alpha_s \int_0^1 dx dy \left[\phi_V(x)\phi_P(y) \left[\frac{1}{\bar{x}(1-\bar{y}x)} + \frac{1}{y^2\bar{x}} \right] - r_\chi^V r_\chi^P \phi_v(x)\phi_p(y) \frac{2}{y\bar{x}} \right], \\
 A_3^i &= \pi\alpha_s \int_0^1 dx dy \left[r_\chi^P \phi_V(x)\phi_P(y) \frac{2\bar{y}}{y\bar{x}(1-\bar{y}x)} - r_\chi^V \phi_P(y)\phi_v(x) \frac{2x}{y\bar{x}(1-\bar{y}x)} \right], \\
 A_3^f &= \pi\alpha_s \int_0^1 dx dy \left[r_\chi^P \phi_V(x)\phi_P(y) \frac{2(1+\bar{x})}{y\bar{x}^2} + r_\chi^V \phi_P(y)\phi_v(x) \frac{2(1+y)}{y^2\bar{x}^2} \right],
 \end{aligned} \tag{5}$$

and $A_1^f = A_2^f = 0$. $\phi_V(x)$ and $\phi_P(y)$ are 2-twist distribution amplitudes, and $\phi_v(x)$ and $\phi_p(y)$ are 3-twist distribution amplitudes for vector and pseudoscalar mesons, respectively. All the terms proportional to r_χ^M are suppressed by power of Λ_{QCD}/m_b in the heavy-quark limit. For pseudoscalar, the ratio r_χ^P is $2m_P^2/m_b(\mu)(m_q + m_{\bar{q}})(\mu)$ and for vector meson it is $2m_V f_V^\perp(\mu)/m_b(\mu)f_V$. The $f_V^\perp(\mu)$ is a tensor decay constant and it is scale dependence [4]. We implement this by using a highly asymmetric D -meson wave function, which is strongly peaked at a light-quark momentum fraction of order Λ_{QCD}/m_D . Hence, we have

$$\phi_D(y) = 6y\bar{y} \left[1 + \sum_{n=1}^{\infty} \alpha_n(\mu) C_n^{3/2}(y-\bar{y}) \right],$$

where $\alpha_1^D = 0.8$ and $\alpha_2^D = 0.4$ ($\alpha_i^D = 0$, $i > 2$); also, $C_1^{3/2}(y - \bar{y}) = 3(y - \bar{y})$ and $C_2^{3/2}(y - \bar{y}) = 15/2(y - \bar{y})^2 - 3/2$. In other words, J/ψ is small in the heavy-quark limit, but its Bohr radius is larger than $1/m_b$. On the other hand, in the limit $m_c/m_b \rightarrow 0$, the J/ψ treats as a light meson relative to the B meson which asymptotic distribution amplitudes have been considered for it in leading twist, i.e., $\phi(x) = \phi_{\parallel}(x) = 6x\bar{x}$. The 3-twist distribution amplitudes are $\phi_p(y) = 1$ for pseudoscalar meson (D) and $\phi_v(x) = 3(x - \bar{x})$ for vector meson (J/ψ).

In heavy-quark effective theory (HQET), below the m_c scale, the vector and tensor currents have the same anomalous dimensions; that is, $f_{J/\psi}^{\perp}$ and $f_{J/\psi} m_c$ scale as the same power. Up to the m_b scale, $f_{J/\psi}^{\perp}$ changes its scale with a factor $[\alpha_s(m_b)/\alpha_s(m_c)]^{4/3\beta}$ and m_c — with $[\alpha_s(m_b)/\alpha_s(m_c)]^{4/\beta}$. Then the ratio $f_{J/\psi}^{\perp}/f_{J/\psi}$ becomes $[\alpha_s(m_b)/\alpha_s(m_c)]^{8/(3\beta)} \times 2m_c(m_b)/m_{J/\psi}$, where $\beta = (11N_c - 2n_f)/3$ and $m_c(m_b)$ is the running mass for charmed quark at scale m_b . However, the scale factor $[\alpha_s(m_b)/\alpha_s(m_c)]^{8/(3\beta)}$ is small and can be ignored [5]. We have ($\mu = m_b$)

$$r_{\chi}^{J/\psi} = 4 \frac{m_c}{m_b}, \quad (6)$$

for J/ψ meson, and

$$r_{\chi}^D = \frac{2m_D^2}{m_b}, \quad (7)$$

for D meson. Also, there are some logarithmic endpoint divergences in weak annihilation kernels. This effect has been parameterized in terms of the divergent integral X_A which models these quantities by using the parameterizations [6]

$$\int \frac{du}{u} \rightarrow X_A. \quad (8)$$

The magnitude of X_A is universal for final states:

$$X_A = \ln \left(\frac{m_B}{\Lambda_{\text{QCD}}} \right) [1 + \rho_A \exp(-i\Phi_A)], \quad (9)$$

where $\rho_A \leq 1$, and Φ_A is an arbitrary strong interaction phase, which may be caused by soft rescattering; this quantity is treated as phenomenological parameter. We have considered two parameters for Λ_{QCD} , e.g., 225 and 500 MeV, which are the QCD scale parameters. For $B^+ \rightarrow J/\psi D^+$ and $B^0 \rightarrow J/\psi D^0$ decays, we first have extracted the contribution of the coefficients in the annihilation amplitudes. The coefficients of annihilation contributions have only been contributed. Hence, in Fig.2, we have shown the Feynman diagrams for $B^+ \rightarrow J/\psi D^+$ decay, which include the b_1 and b_2 coefficients, and for $B^0 \rightarrow J/\psi D^0$ decay, where the b_1 coefficient is participated in decay amplitude. In these decays, there is not penguin annihilation contribution. So, we have

$$\begin{aligned} A(B^+ \rightarrow J/\psi D^+) &= \frac{G_F}{\sqrt{2}} f_B f_D f_{J/\psi} [V_{ud} V_{cb}^* b_1 + V_{cd} V_{ud}^* b_2], \\ A(B^0 \rightarrow J/\psi D^0) &= \frac{G_F}{\sqrt{2}} f_B f_D f_{J/\psi} [V_{ud} V_{cb}^* b_1]. \end{aligned} \quad (10)$$

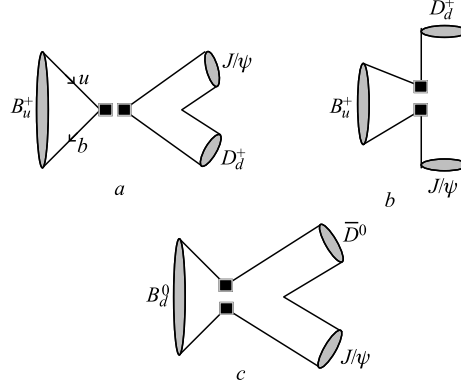


Fig. 2. The Feynman diagrams for $B^+ \rightarrow J/\psi D^+$ (a, b) and $B^0 \rightarrow J/\psi D^0$ (c) decays

The branching ratios are given by

$$\text{BR}(B \rightarrow J/\psi D) = \frac{P_c^3 \tau_B}{8\pi m_{J/\psi}^2} \left| \frac{A(B \rightarrow J/\psi D)}{\varepsilon \cdot P_B} \right|^2, \quad (11)$$

where τ_B , $A(B \rightarrow J/\psi D)$, and ε are the life time of B meson, decay amplitude, and polarization vector for J/ψ , respectively. Also, P_c is the centre-of-mass momentum of mesons

$$P_c = \frac{\sqrt{[m_B^2 - (m_D + m_{J/\psi})^2][m_B^2 - (m_D - m_{J/\psi})^2]}}{2m_B}.$$

1.2. Input Parameters. Here, we have introduced the essential input quantities:

$$m_b(\mu = m_b) = 4.4 \text{ GeV}, \quad m_c = 1.45 \text{ GeV}, \quad m_B = 5.28 \text{ GeV},$$

$$m_D = 1.867 \text{ GeV}, \quad m_{J/\psi} = 3.1 \text{ GeV}, \quad \alpha_s(\mu = m_b) = 0.22,$$

$$f_{J/\psi} = 405 \text{ MeV}, \quad f_B = 190 \text{ MeV}, \quad f_D = 222 \text{ MeV},$$

$$N_c = 3, \quad C_F = \frac{N^2 - 1}{2N}, \quad G_F = 1.166 \cdot 10^{-5}.$$

Also, we have used the next-to-leading Wilson coefficients calculated in the naive dimensional regularization (NDR) scheme and at m_b scale. It is given by [7]

$$C_1 = 1.082, \quad C_2 = -0.185, \quad C_3 = 0.014, \quad C_4 = -0.035, \quad C_5 = 0.009, \quad C_6 = -0.041,$$

$$C_7/\alpha = -0.002, \quad C_8/\alpha = 0.054, \quad C_9/\alpha = -1.292, \quad C_{10}/\alpha = 0.263,$$

where $\alpha = 1/129$. We also have used the Wolfenstein parameterization for CKM matrix elements [8]:

$$\begin{pmatrix} V_{ud} & V_{us} & V_{ub} \\ V_{cd} & V_{cs} & V_{cb} \\ V_{td} & V_{ts} & V_{tb} \end{pmatrix} = \begin{pmatrix} 1 - \lambda^2/2 & \lambda & A\lambda^3(\rho - i\eta) \\ -\lambda & 1 - \lambda^2/2 & A\lambda^2 \\ A\lambda^3(1 - \rho - i\eta) & -A\lambda^2 & 1 \end{pmatrix},$$

where $|V_{cb}| = 0.0413$, $\lambda = 0.22$, $\bar{\eta} = 0.33$ and

$$\bar{\rho} = \rho \left(1 - \frac{\lambda^2}{2}\right), \quad \bar{\eta} = \eta \left(1 - \frac{\lambda^2}{2}\right),$$

and the experimental life times for B^0 and B^\pm are [9]

$$\begin{aligned} \tau_{B^\pm} &= (1.638 \pm 0.011) \cdot 10^{-12} S, \\ \tau_{B^0} &= (1.525 \pm 0.009) \cdot 10^{-12} S. \end{aligned}$$

2. DISCUSSION

In this paper, we have computed branching ratios for $B^+ \rightarrow J/\psi D^+$ and $B^0 \rightarrow J/\psi D^0$ decays. These decays have only annihilation contributions. The annihilation amplitudes for each decay are studied in the different hadronic scales. On the other hand, they have been calculated in the different parameters of X_A , which play a significant role in our results.

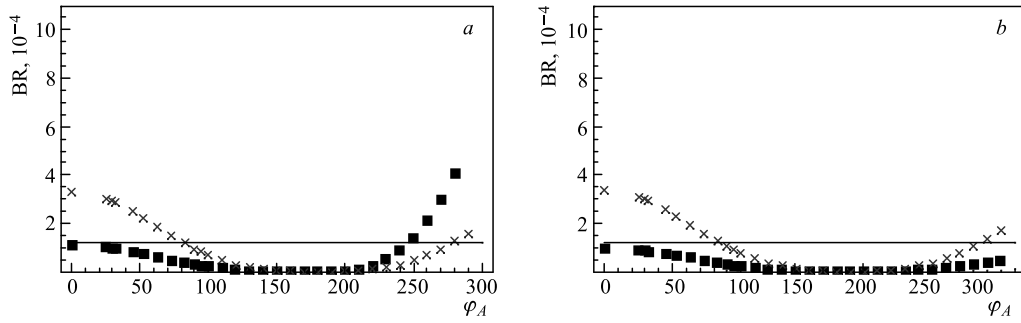


Fig. 3. The obtained data correspond to $B^+ \rightarrow J/\psi D^+$ for $\rho_A = 1$ (a), $\rho_A = 1/2$ (b) (squares — for $\Lambda = 225$ MeV, crosses — for $\Lambda = 500$ MeV, the solid line — for experimental data $< 1.2 \cdot 10^{-4}$)

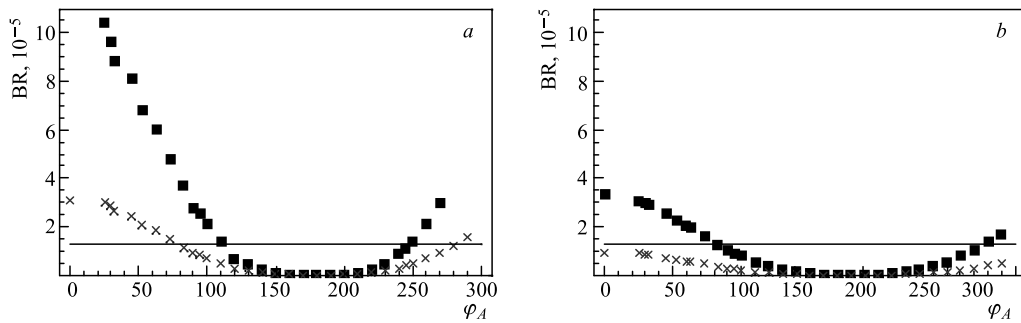


Fig. 4. The obtained data correspond to $B^0 \rightarrow J/\psi D^0$ for $\rho_A = 1$ (a), $\rho_A = 1/2$ (b) (squares — for $\Lambda = 225$ MeV, crosses — for $\Lambda = 500$ MeV, the solid line — for experimental data $< 1.3 \cdot 10^{-5}$)

Table 1. Branching ratios for $B^+ \rightarrow J/\psi D^+$
($\Lambda = 225$ MeV)

ρ	$\Phi_A, ^\circ$	BR, 10^{-4}
0	$0 \sim 360$	$0.05^{+0.003}_{-0.002}$
1	0	$1.11^{+0.01}_{-0.002}$
	30	$0.97^{+0.01}_{-0.003}$
	240	$0.87^{+0.004}_{-0.002}$
	250	$1.41^{+0.01}_{-0.0001}$
$\frac{1}{2}$	83	$1.28^{+0.002}_{-0.001}$
	90	$1.06^{+0.001}_{-0.001}$
	270	$1.06^{+0.01}_{-0.001}$
	280	$1.37^{+0.01}_{-0.001}$
Exp.		< 1.2

Table 2. Branching ratios for $B^+ \rightarrow J/\psi D^+$
($\Lambda = 500$ MeV)

ρ	$\Phi_A, ^\circ$	BR, 10^{-4}
0	$0 \sim 360$	$0.547^{+0.002}_{-0.002}$
1	110	$1.39^{+0.05}_{-0.1}$
	120	$0.68^{+0.04}_{-0.06}$
	240	$0.86^{+0.03}_{-0.05}$
	250	$1.39^{+0.01}_{-0.02}$
$\frac{1}{2}$	83	$1.26^{+0.02}_{-0.02}$
	95	$0.91^{+0.01}_{-0.02}$
	260	$0.78^{+0.01}_{-0.01}$
	280	$1.36^{+0.01}_{-0.007}$
Exp.		< 1.3

Table 3. Branching ratios for $B^0 \rightarrow J/\psi D^0$
($\Lambda = 225$ MeV)

ρ	$\Phi_A, ^\circ$	BR, 10^{-5}
0	$0 \sim 360$	$0.547^{+0.002}_{-0.001}$
1	110	$1.39^{+0.05}_{-0.1}$
	120	$0.68^{+0.04}_{-0.06}$
	240	$0.86^{+0.03}_{-0.05}$
	250	$1.39^{+0.01}_{-0.02}$
$\frac{1}{2}$	83	$1.26^{+0.02}_{-0.02}$
	95	$0.91^{+0.01}_{-0.02}$
	260	$0.78^{+0.01}_{-0.01}$
	280	$1.36^{+0.01}_{-0.007}$
Exp.		< 1.3

Table 4. Branching ratios for $B^0 \rightarrow J/\psi D^0$
($\Lambda = 500$ MeV)

ρ	$\Phi_A, ^\circ$	BR, 10^{-5}
0	$0 \sim 360$	$0.135^{+0.001}_{-0.001}$
1	83	$1.17^{+0.001}_{-0.02}$
	95	$0.82^{+0.001}_{-0.002}$
	270	$0.96^{+0.01}_{-0.002}$
	280	$1.2^{+0.01}_{-0.004}$
$\frac{1}{2}$	0	$0.96^{+0.004}_{-0.007}$
	30	$0.86^{+0.005}_{-0.001}$
	280	$0.39^{+0.001}_{-0.02}$
	290	$0.50^{+0.003}_{-0.006}$
Exp.		< 1.3

The X_A has been concluded from the divergence integrals in hard-scattering kernels and appeared in Eq. (10) which can be changed in definite intervals. Here, we have changed three effective variables in X_A , including: Λ , ρ_A , and φ_A . We have chosen arbitrary phases for φ_A and ρ_A in this parameter, which have the better results for our calculations. By considering that $\Lambda = 225$ and 500 MeV, our results are given in Tables 1–4 for $B^+ \rightarrow J/\psi D^+$ and $B^0 \rightarrow J/\psi D^0$ which are the best results in below the upper bound data of these decays. These data are plotted in Figs. 3 and 4. We have tried to decrease the discrepancy between theoretical results and experimental data. It has shown, we could find that the most of the obtained branching ratios for $B^+ \rightarrow J/\psi D^+$ and $B^0 \rightarrow J/\psi D^0$ are placed in the experimental range for $\Lambda = 225$ MeV and $\Lambda = 500$ MeV. In [3], the branching ratio is calculated in pQCD approach, which is given to be $(3.45^{+1.22}_{-1.46} \pm 1.51 \pm 0.32) \cdot 10^{-6}$ for $B^0 \rightarrow J/\psi D^0$. The upper bounds of experimental data on $B^+ \rightarrow J/\psi D^+$ and $B^0 \rightarrow J/\psi D^0$ decays are $1.2 \cdot 10^{-4}$ and $1.3 \cdot 10^{-5}$, respectively [9].

REFERENCES

1. Arnesen C. M., Rothstein I. Z., Stewart I. W. // Phys. Lett. B. 2007. V. 647. P. 405.
2. Beneke M. et al. // Nucl. Phys. B. 2001. V. 606. P. 245.
3. Li Y., Lu C. D., Qiao C. F. // Phys. Rev. D. 2006. V. 73. P. 094006.
4. Beneke M., Neubert M. // Nucl. Phys. B. 2003. V. 675. P. 333.
5. Cheng H. Y., Keum Y. Y., Yang K. C. // Phys. Rev. D. 2002. V. 65. P. 094023.
6. Beneke M., Rohrer J., Yang D. // Nucl. Phys. B. 2007. V. 774. P. 64.
7. Buchalla G., Buras A. J., Lautenbacher M. E. // Rev. Mod. Phys. 1996. V. 68. P. 1125.
8. Wolfenstein L. // Phys. Rev. Lett. 1983. V. 51. P. 1945.
9. Nakamura K. et al. Particle Data Group // J. Phys. G. 2010. V. 37. P. 075021.

Received on January 22, 2013.